Targeting Streptococcus salivarius in Peri-Implantitis:

Two Antimicrobial and Antibiofilm Peptides

Samia Chergui*, S. Thomas*, M. Daggett*, B. Mattingly*, and J. F. Treml*†

Peri-implantitis, a persistent complication associated with dental implants, is driven by complex, antibiotic-resistant oral biofilms. Antimicrobial Peptides (AMPs) may represent novel, safe, and effective therapies against Streptococcus salivarius, a key early colonizer in peri-implant biofilms. S. salivarius was isolated and identified by 16S sequencing from human saliva, followed by standardized growth and biofilm assays to establish a physiologically relevant testing model. RR12 is a novel peptide that was rationally designed, synthesized, and characterized for structural integrity for comparison against KR12, a natural LL-37 derivative known to be effective against bacteria. Both peptides demonstrated dose-dependent inhibition of S. salivarius biofilm formation, but KR12 consistently achieved superior antimicrobial and antibiofilm effects with lower cytotoxicity. These findings underscore the necessity of biological validation in peptide development and support the use of AMPs as promising alternatives to traditional antibiotics. AMP-based coatings and gels for dental implants could offer localized, resistance-proof infection control.

The widespread adoption of dental implants has transformed restorative dentistry, offering functional and aesthetic solutions for tooth loss.[1] However, their long-term success is increasingly compromised by peri-implantitis—a chronic inflammatory condition associated with bone loss and implant failure.[2] Central to this disease is the rapid colonization of implant surfaces by oral biofilms, which confer resistance to host defenses and antibiotics.[3,4] Among these biofilm-forming organisms, Streptococcus salivarius plays a pivotal role as an early colonizer, facilitating the adhesion of pathogenic species and contributing to biofilm maturation.[4,5]

The biofilm matrix not only acts as a mechanical barrier but also promotes horizontal gene transfer and antimicrobial resistance.[6] Consequently, standard interventions like debridement or antibiotics often fail to fully eradicate the infection.[7] This has led to growing interest in antimicrobial peptides (AMPs), which possess broad-spectrum activity, low resistance potential, and biofilm-disrupting capabilities.[8,9] AMPs derived from human cathelicidins, particularly LL-37, have inspired the development of synthetic analogs with improved selectivity and reduced cytotoxicity.[5,10]

*University of Kansas, Edwards Campus, Biotechnology

†Corresponding Author jtreml@ku.edu

This study investigates the design and functional characterization of a novel AMP, RR12, as a targeted strategy against S. salivarius. The performance of RR12 was compared to KR12—a validated LL-37 fragment—with emphasis on antimicrobial efficacy, biofilm inhibition, and cytotoxicity. Our findings support the use of engineered AMPs in next-generation dental therapeutics and highlight the translational potential of AMP-based coatings for peri-implantitis control.

Materials and Methods

Bacterial Isolation

Saliva samples were collected from healthy adult volunteers and immediately streaked onto Mitis Salivarius Agar plates (Sigma-Aldrich, Cat. No. 01337-500G-F) to selectively isolate *Streptococcus* species. Plates were incubated at 37°C for 24 hours. To ensure purity, single colonies with distinct morphologies were subcultured onto fresh Mitis Salivarius Agar. Each colony was characterized by Gram staining and catalase testing using standard protocols. For genomic analysis, a single colony from each morphology was inoculated into 5 mL Luria-Bertani (LB) Broth (Fisher BioReagents, Cat. No. BP9723-500) and grown overnight at 37°C with shaking. Genomic DNA was isolated from these cultures using a heat shock method: 1 mL of culture was centrifuged, the pellet was resuspended in 100 µL PBS, heated at 95°C for 10 minutes, and centrifuged again to recover the supernatant containing DNA. PCR amplification of the 16S rRNA gene was performed using universal primers 27F and 1492R, with commercial *S. salivarius* DNA (provided by M. Daggett) as a positive control and a no-template reaction as a negative control. PCR products were separated on a 1% agarose gel (Fisher BioReagents, Cat. No. BP1356-500), excised, and purified using the Monarch DNA Gel Extraction Kit (New England Biolabs, Lot#0051612). Purified PCR products were submitted to Eurofins Genomics for 16S rRNA sequencing to confirm bacterial identity.

AMP Design

Antimicrobial peptide sequences were electronically submitted to the University of Kansas Medical Center Synthetic Chemical Biology Core Facility for synthesis. Physicochemical properties, including net charge, hydrophobicity, and CPP potential, were analyzed using the CellPPD web server. Three-dimensional structural models of the peptides were generated and visualized using UCSF ChimeraX.

pH Tolerance Assay

To assess environmental adaptation, *S. salivarius* was cultured in tryptic soy broth Tryptic Soy Broth (Fisher scientific LOT# 1306492) adjusted to various pH levels using sterile-filtered HCl or NaOH. Media

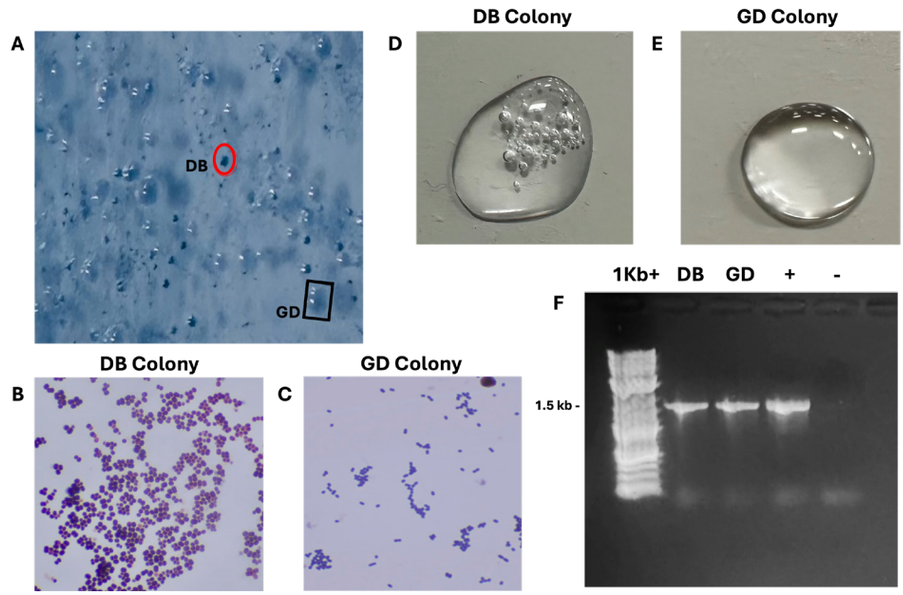

Figure 1 | Phenotypic and molecular identification of oral bacterial colonies isolated from human saliva.
(A) Distinct colony morphologies appear on Mitis Salivarius Agar after overnight incubation. Dark blue colonies (DB) and gumdrop-like colonies (GD) are visually distinguishable and selected for further analysis.
(B&C) Gram staining shows cocci in clusters for DB (**B**), consistent with Staphylococcus spp., and cocci in chains for GD (**C**), characteristic of Streptococcus spp. Both stain purple, indicating Gram-positive cell walls.
(D&E) Catalase testing reveals bubble formation in DB colonies (**D**, Catalase+), while GD colonies show no reaction (**E**, Catalase–), supporting preliminary genus-level classification.
(D) PCR amplification of the 16S rRNA gene yields ~1.5 kb amplicons for both isolates. Sanger sequencing and BLAST analysis identify DB as Staphylococcus haemolyticus and GD as Streptococcus salivarius, confirming phenotypic observations.

were autoclaved post-adjustment. Overnight cultures were inoculated into each pH-adjusted broth and incubated at 37°C for 12-18 hours. Growth was quantified by optical density at 600 nm (OD_{600}) using a spectrophotometer and SpectraMax software.

Growth Monitoring and Bacterial Enumeration

S. salivarius was cultured in tryptic soy broth (TSB) and incubated at 37 °C under aerobic conditions for 36 hours. Bacterial growth was monitored at multiple time points 0, 6, 12, 24, and 36 hours) by measuring optical density at OD_{600} using a spectrophotometer.
Once cultures reached an OD_{600} of approximately 0.9, a series of ten-fold serial dilutions were prepared in sterile PBS. For bacterial enumeration, 100 µL from each dilution was plated onto LB agar plates in triplicate and incubated overnight at 37 °C. Colony-forming units per milliliter (CFU/mL) were calculated by counting visible colonies and accounting for the dilution factor.
To establish a correlation between OD_{600} and bacterial concentration, the CFU values were plotted against the corresponding OD readings from the TSB cultures. This standard curve was used to normalize bacterial input across subsequent experimental assays.

Optical Density Assay

Antimicrobial activity of RR12 and KR12 was evaluated using a 96-well microplate OD assay. Peptides were prepared at various concentrations in TSB. An overnight S. salivarius culture was diluted to OD_{600} = 0.3. For each assay, 100 µL of standardized bacteria and 100 µL peptide solution were added per well (triplicates). Ampicillin powder (Alfa Aesar, Cat. No. J60977.06) served as a positive control; bacteria-only wells served as negative controls. Initial OD_{600} was measured at t=0. Plates were incubated overnight at 37°C with shaking at 200 rpm, and OD_{600} was measured again after 12 hours.

Biofilm Formation Assay

Biofilm formation was quantified using the same 96-well plates post-OD assay. Media and non-adherent bacteria were gently aspirated, and wells were washed twice with 200 µL PBS. The wells were air-dried and stained with 100 µL 0.1% crystal violet (Fisher Scientific, Cat. No. C581-100) for 20 minutes. Excess stain was removed by washing three times with PBS, and plates were air-dried. Crystal violet was solubilized with 150 µL methanol (Fisher Scientific, Cat. No. A452-4) per well for 15 minutes. Absorbance was measured at 595 nm. All assays were performed in triplicates, with ampicillin as a positive control and uninoculated media as a negative control. This assay was not done in triplicates at the time of publication.

Cytotoxicity Assay

KR12 and RR12 cytotoxicity against mammalian cells was assessed using an MTT assay on HCT116 colon carcinoma cells. Cells were maintained in DMEM with 10% FBS and 1% penicillin-streptomycin. HCT116 cells were seeded into 96-well plates and allowed to adhere overnight. Peptides were added at various concentrations and incubated for 24 hours at 37°c. MTT reagent (0.5 mg/mL) was added and incubated 3–4 hours. Formazan crystals were dissolved in 100uL DMSO, and absorbance at 490 nm was measured to determine cell viability.

Results

Isolation and Identification of Streptococcus salivarius

Saliva samples were streaked onto Mitis Salivarius Agar and incubated overnight resulting in two distinct colony morphologies: one gumdrop-like and one dark blue (**Figure 1A**). Gram staining showed that the gumdrop colony consisted of Gram-positive cocci in chains, while the dark blue colony consisted of Gram-positive cocci in clusters (**Figure 1B&C**). The dark blue colony was catalase-positive, and the gumdrop colony was catalase-negative **(Figure 1D&E).**
The PCR amplification of the 16S rRNA gene, yielded ~1.5 kb bands for both colony types (**Figure 1F**) which are consistent

for the predicted size of the gene of interest. PCR amplicons were purified from the gen and sent for Sanger sequencing. BLAST analysis identified the gumdrop colony as *S. salivarius* (Score: 1563, E-value: 0, Accession: MZ824593.1) and the dark blue colony as *Staphylococcus haemolyticus* (Score: 693, E-value: 0, Accession: MH542264.1). These identifications are consistent with the test results above.

pH Tolerance of Streptococcus salivarius

The pH tolerance assay showed that S. salivarius exhibited optimal growth in media adjusted to pH 7–8. The highest optical density values were recorded at these pH levels. Growth was still detectable at more acidic or basic pH values but was markedly reduced compared to neutral and slightly alkaline conditions. **(Figure 2A)**

Growth Kinetics and Standardization of S. salivarius Inoculum

The growth curve (**Figure 2B**) shows that *S. salivarius* enters exponential phase between 6- and 12-hours post-inoculation and reaches stationary phase by 24 hours, indicating this is the optimal window for antimicrobial exposure when cells are most metabolically active. Additionally, a standard curve correlating optical density at 600 nm with colony-forming units per milliliter (CFU/mL) (**Figure 2C**) demonstrates a strong linear relationship. This correlation is used to normalize bacterial input across experiments and ensure consistent starting concentrations for all treatments.

Antimicrobial Peptide Design

KR12, derived from human cathelicidin LL-37, exhibits strong antimicrobial and anti-biofilm activity due to its amphipathic α-helical structure and positive charge.[11] Key features such as amphipathicity, cationic charge, and hydrophobic residues are essential for disrupting bacterial membranes and biofilms.[12] To improve these properties, RR12 was designed by increasing lysine content to enhance charge and salt resistance while preserving the α-helical scaffold critical for membrane interaction. Structural modeling with ChimeraX confirmed that both peptides maintain their α-helical conformations, vital for antimicrobial function (**Figure 3A&B**). These findings align with studies showing that optimizing charge and helical structure improves peptide potency and selectivity.[13]

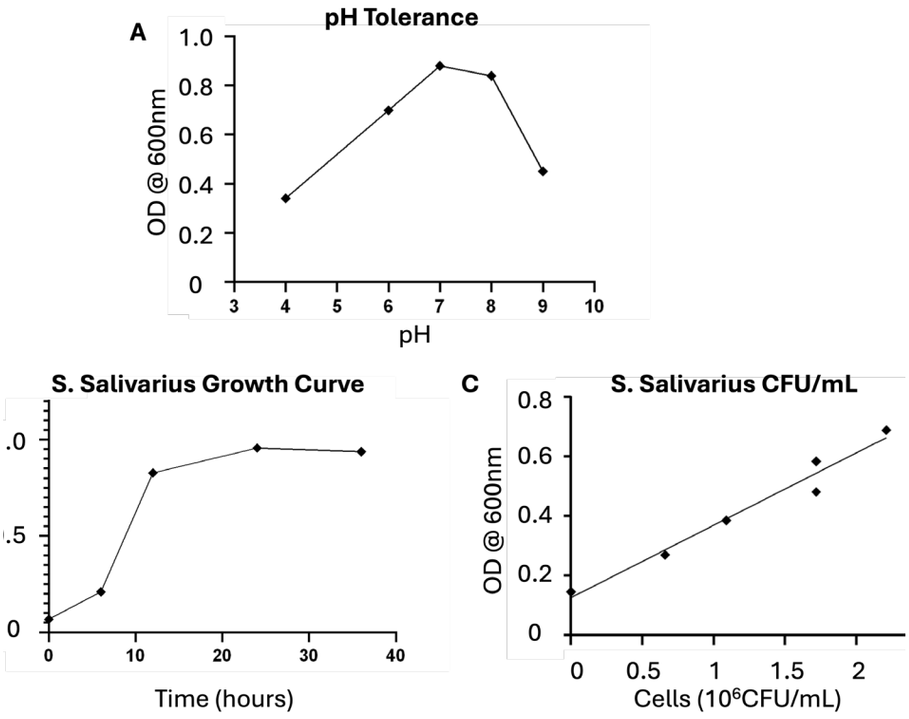

Figure 2 | Physiological characterization of Streptococcus salivarius under simulated oral conditions.

(A) S. salivarius exhibits optimal growth at neutral to slightly alkaline pH, as determined by measuring optical density at 600 nm after 18–24 hours of incubation. Growth decreases significantly at more acidic or basic conditions.

(B) The bacterial growth curve demonstrates that S. salivarius enters exponential phase between 6–12 hours post-inoculation, with stationary phase reached by 24 hours. The 6-12 hour time point is selected for antimicrobial assays to capture peak metabolic activity.

(C) A standard curve establishes a linear correlation between OD_{600} and colony-forming units per milliliter (CFU/mL), allowing accurate standardization of bacterial input in all experimental wells.

Antimicrobial Activity of KR12 and RR12

A dose-dependent inhibition of *S. salivarius* was observed for both KR12 and RR12 peptides (**Figure 4A**). At lower concentrations (10–313 µg/mL), both peptides exhibited minimal inhibition, with percent inhibition values close to zero or slightly negative. As the concentration increased, KR12 showed a marked increase in antimicrobial activity, achieving nearly complete inhibition at concentrations of 625 µg/mL and above. RR12 demonstrated only modest inhibition across all concentrations, with percent inhibition remaining below 40% until the highest dose tested. At 1250 µg/mL and 2500 µg/mL, both peptides resulted in complete growth inhibition.

Inhibition of S. salivarius Biofilm Formation

Biofilm quantification using the crystal violet assay showed that both KR12 and RR12 peptides reduced S. salivariusbiofilm formation in a concentration-dependent manner (**Figure 4B**). At lower concentrations (10–156.5 µg/mL), there was no statistically significant reduction in biofilm biomass for either peptide. At 312.5 µg/mL and above, KR12 showed a marked and statistically significant decrease in biofilm formation compared to RR12. At the highest concentrations tested (1250 and 2500 µg/mL), KR12 virtually eliminated biofilm formation, while RR12-treated wells retained higher OD values, indicating less effective biofilm inhibition. Visual inspection of the stained plates supported these quantitative findings (**Figure 4C**).

Cytotoxicity of RR12 and KR12 on HCT116 Cells

Both peptides exhibited a concentration-dependent reduction in HCT116 human colon carcinoma cells viability (**Figure 5A**). At concentrations up to 375 µg/mL, cell viability remained above 70% for both peptides, with no statistically significant difference. At 750 µg/mL and above, a marked decrease in cell viability was observed, particularly for KR12. At concentrations of 1500 µg/mL and higher, KR12 induced a significantly greater reduction in cell viability compared to RR12, with viability dropping below 30% for both peptides at the highest concentrations tested. Visual inspection of the stained plates supported these quantitative findings (**Figure 5B**).

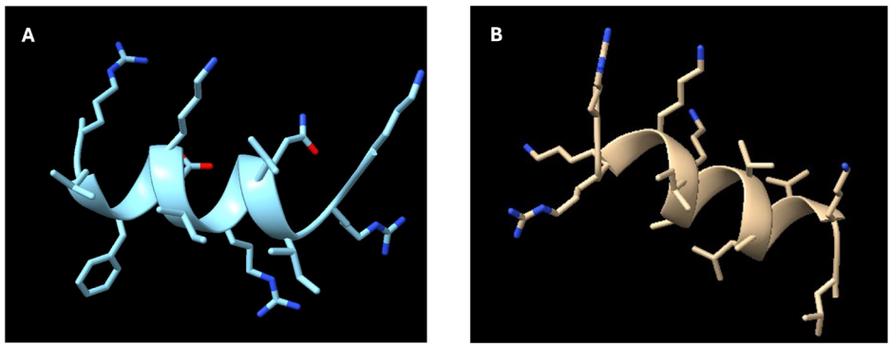

Figure 3 | Structural and physicochemical features of antimicrobial peptides KR12 and RR12. (A) KR12 (KRIVQRIKDFLR) and **(B)** RR12 (RRKKIAKVALVK) are engineered cell-penetrating peptides (CPPs) derived from LL-37. Both peptides form amphipathic helices essential for membrane disruption. KR12 carries a net charge of +4, with moderate hydrophilicity (0.73) and a molecular weight of 1.57 kDa. In contrast, RR12 is more cationic (+6), more hydrophilic (0.87), and slightly smaller (1.41 kDa).

Discussion

This study demonstrates the promise and challenges of using engineered antimicrobial peptides (AMPs) as targeted agents against early oral biofilm colonizers implicated in peri-implantitis. By systematically isolating and confirming *S. salivarius* from human saliva, we established a clinically relevant model for evaluating antibiofilm strategies. The pH tolerance profile of *S. salivarius* confirmed its adaptation to oral conditions and validated the physiological relevance of our in vitro assays.

Both RR12 and KR12 peptides exhibited dose-dependent inhibition of *S. salivarius* planktonic growth and biofilm formation, with KR12 consistently showing superior efficacy. The observed hormesis effect at low concentrations—where sub-inhibitory doses had little or even slightly stimulatory effects—underscores the complexity of AMP-bacteria interactions and the importance of precise dosing.[11] At higher concentrations, KR12 nearly eradicated both planktonic bacteria and biofilms, while

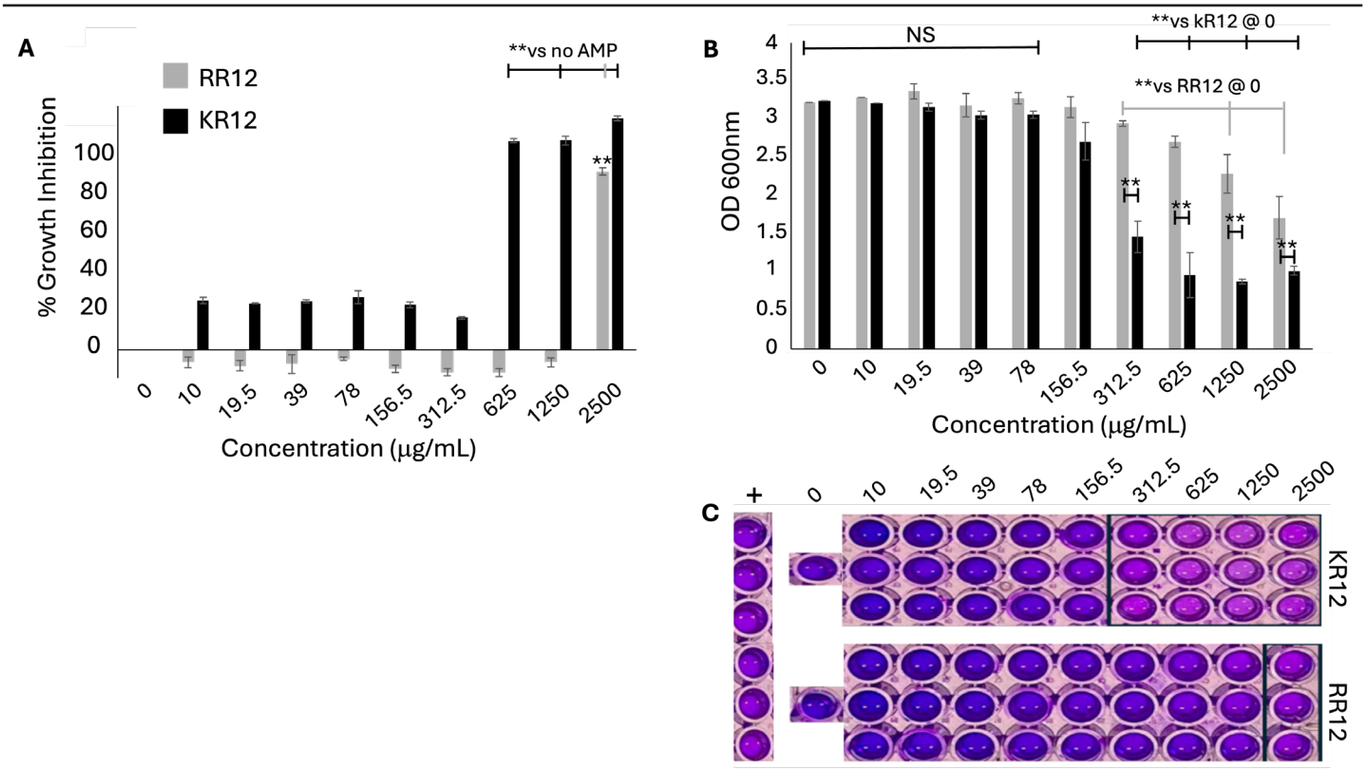

Figure 4 | Antimicrobial and antibiofilm activity of KR12 and RR12 peptides against Streptococcus salivarius. **(A)** Percent inhibition of S. salivarius growth following treatment with increasing concentrations of KR12 and RR12 (10–2500 µg/mL), assessed via OD_{600} after 12 hours. **(B)** Quantification of biofilm biomass using crystal violet staining and absorbance at 600 nm after peptide exposure. **(C)** Representative images of stained 96-well plates show biofilm retention following peptide treatment. Ampicillin (+) and untreated bacteria (–) serve as positive and negative controls, respectively. Data are presented as mean ± standard deviation; statistical significance is indicated.

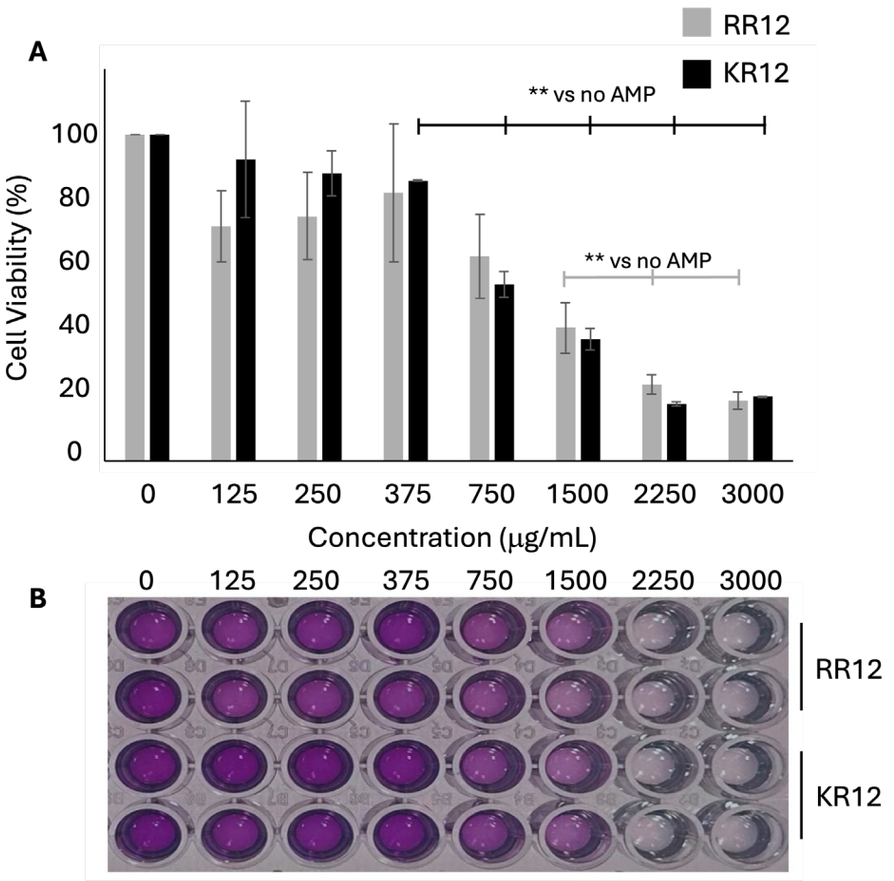

Figure 5 | Cytotoxicity of KR12 and RR12 peptides on HCT116 cells assessed by MTT assay.

(A) Cell viability (%) of HCT116 human colon carcinoma cells treated with increasing concentrations of KR12 and RR12 peptides (0–3000 µg/mL) for 24 hours. Viability is quantified using MTT reduction and expressed relative to untreated controls.

(B) Representative image of 96-well plates post-MTT assay showing the intensity of formazan staining across the concentration range for each peptide.

RR12 achieved only partial inhibition under similar conditions.

Cytotoxicity assays revealed that both peptides were relatively well-tolerated by mammalian cells at concentrations effective against bacteria, but KR12 displayed cytotoxicity at higher doses. This finding highlights the central challenge that even synthetically derived AMPs must balance antimicrobial potency with host cell compatibility to ensure clinical safety.

Taken together, these results support the potential of AMPs—particularly KR12—as promising alternatives or adjuncts to traditional antibiotics for the prevention and treatment of peri-implantitis. Their ability to disrupt early biofilm formation and overcome some limitations of conventional antimicrobials is especially relevant in an era of rising antibiotic resistance. However, the therapeutic window must be carefully optimized to maximize efficacy while minimizing cytotoxicity.

Future Directions

Future work should focus on peptide optimization for improved selectivity, in vivo validation using relevant animal models, and the development of delivery systems such as implant coatings or local gels. As AMPs move closer to clinical translation, their integration into dental practice could offer a new paradigm for biofilm management and implant longevity.

Acknowledgments

I would like to express my sincere gratitude to Dr. Jack Treml for his outstanding mentorship and guidance throughout the course of this research. I am also deeply thankful to Dr. Mattingly, Dr. Thomas, and Dr. Dagget for their support and insightful feedback, which greatly enriched the development of this work.

Special thanks to my classmate Kuljet for generously providing HCT116 human colon carcinoma cells, and to the University of Kansas and JCERT for their institutional support.

This research was funded in part by the KU Edwards Research Grant, with additional generous support from Catalent, Hill's Pet Nutrition and ICON.

Author's Biography

Samia Chergui is a senior in the Biotechnology program at the University of Kansas Edwards Campus. Upon completing her undergraduate degree, she plans to enter the biotechnology industry to gain hands-on research experience before choosing a focus for her Ph.D. studies. Her primary academic interests lie in immunology and genetics.

Author Contributions

S.C. contributed to the experimental work, design, and writing of this work; B.M., S.T., M.D., and J.F.T contributed to the design and editing of this work.

References

1. Berger, D., Rakhamimova, A., Pollack, A. & Loewy, Z. Oral Biofilms: Development, Control, and Analysis. High-Throughput 7, 24 (2018).
2. Körtvélyessy, G., Tarjányi, T., Baráth, Z. L., Minarovits, J. & Tóth, Z. Bioactive coatings for dental implants: A review of alternative strategies to prevent peri-implantitis induced by anaerobic bacteria. Anaerobe 70, 102404 (2021).
3. Roger, P., Delettre, J., Bouix, M. & Béal, C. Characterization of Streptococcus salivarius growth and maintenance in artificial saliva. J. Appl. Microbiol. 111, 631–641 (2011).
4. Patras, K. A. et al. Streptococcus salivarius K12 Limits Group B Streptococcus Vaginal Colonization. Infect. Immun. 83, 3438–3444 (2015).
5. Zhuo, H., Zhang, X., Li, M., Zhang, Q. & Wang, Y. Antibacterial and Anti-Inflammatory Properties of a Novel Antimicrobial Peptide Derived from LL-37. Antibiot. Basel Switz. 11, 754 (2022).
6. Vertillo Aluisio, G. et al. Streptococcus salivarius 24SMBc Genome Analysis Reveals New Biosynthetic Gene Clusters Involved in Antimicrobial Effects on Streptococcus pneumoniae and Streptococcus pyogenes.

Microorganisms 10, 2042 (2022).
7. Wang, Z., Shen, Y. & Haapasalo, M. Antibiofilm peptides against oral biofilms. J. Oral Microbiol. 9, 1327308 (2017).
8. Khurshid, Z. et al. Oral antimicrobial peptides: Types and role in the oral cavity. Saudi Pharm. J. SPJ Off. Publ. Saudi Pharm. Soc. 24, 515–524 (2016).
9. Li, J. et al. Membrane Active Antimicrobial Peptides: Translating Mechanistic Insights to Design. Front. Neurosci. 11, 73 (2017).
10. Calabrese, E. J. & Mattson, M. P. Hormesis provides a generalized quantitative estimate of biological plasticity. J. Cell Commun. Signal. 5, 25–38 (2011).
11. Mahlapuu, M., Håkansson, J., Ringstad, L. & Björn, C. Antimicrobial Peptides: An Emerging Category of Therapeutic Agents. Front. Cell. Infect. Microbiol. 6, 194 (2016).
12. Nguyen, L. T., Haney, E. F. & Vogel, H. J. The expanding scope of antimicrobial peptide structures and their modes of action. Trends Biotechnol. 29, 464–472 (2011).
13. Fjell, C. D., Hiss, J. A., Hancock, R. E. W. & Schneider, G. Designing antimicrobial peptides: form follows function. Nat. Rev. Drug Discov. 11, 37–51 (2011).
14. Castillo-Juárez, I., Blancas-Luciano, B. E., García-Contreras, R. & Fernández-Presas, A. M. Antimicrobial peptides properties beyond growth inhibition and bacterial killing. PeerJ 10, e12667 (2022).